

"Two-dimensional metal dicyanamide frameworks of
BeTriMe[M(dca)₃(H₂O)] (BeTriMe= benzyltrimethylammonium;
dca=dicyanamide; M=Mn²⁺, Co²⁺, Ni²⁺): coexistence of polar and
magnetic orders and nonlinear optical threshold temperature sensing"

by Mirosław Mączka et al.

Table S1. Experimental details

	(I)	(II)	(III)	(IV)
Crystal data				
Chemical formula	C ₁₆ H ₁₈ MnN ₁₀ O	C ₁₆ H ₁₈ MnN ₁₀ O	C ₁₆ H ₁₈ CoN ₁₀ O	C ₁₆ H ₁₈ NiN ₁₀ O
M_r	421.34	421.34	425.33	425.11
Crystal system, space group	Orthorhombic, <i>Pna2</i> ₁	Orthorhombic, <i>Pna2</i> ₁	Orthorhombic, <i>Pna2</i> ₁	Orthorhombic, <i>Pna2</i> ₁
Temperature (K)	295	120	295	250
a, b, c (Å)	17.0942 (7), 8.7146 (3), 13.7283 (5)	16.9085 (3), 8.6712 (2), 13.4009 (3)	16.9433 (7), 8.5926 (3), 13.6148 (5)	16.8309 (6), 8.5268 (4), 13.5078 (6)
V (Å ³)	2045.09 (13)	1964.80(6)	1982.14(13)	1938.55 (13)
Z	4	4	4	4
Radiation type	Mo $K\alpha$	Mo $K\alpha$	Mo $K\alpha$	Mo $K\alpha$
μ (mm ⁻¹)	0.67	0.67	0.90	1.03
Crystal size (mm)	0.23 × 0.18 × 0.09	0.23 × 0.18 × 0.09	0.16 × 0.11 × 0.08	0.18 × 0.11 × 0.07
Data collection				
Diffractometer	Xcalibur, Atlas	Xcalibur, Atlas	Xcalibur, Atlas	Xcalibur, Atlas
Absorption correction	Multi-scan	Multi-scan	Multi-scan	Multi-scan
No. of measured, independent and observed	34020, 4169, 3617	48113, 4017, 3866	19035, 4036, 3636,	15003, 3698, 2710
$[I > 2\sigma(I)]$ reflections				
R_{int}	0.044	0.040	0.024	0.060
$(\sin \theta/\lambda)_{max}$ (Å ⁻¹)	0.625	0.625	0.625	0.625
Refinement				
$R[F^2 > 2\sigma(F^2)], wR(F^2), S$	0.036, 0.088, 1.03	0.021, 0.051, 1.07	0.029, 0.074, 0.83	0.043, 0.068, 1.04
No. of reflections	4169	4017	4036	3698
No. of parameters	264	258	264	258
No. of restraints	25	1	25	1
H-atom treatment	H-atom parameters constrained	H-atom parameters constrained	H-atom parameters constrained	H-atom parameters constrained
$\Delta_{max}, \Delta_{min}$ (e Å ⁻³)	0.36, -0.25	0.16, -0.14	0.410, -0.230	0.27, -0.25
Absolute structure determined using	Flack x 1507 quotients [(I+)-(I-)]/[I+(I-)] ^[1]	1778 quotients [(I+)-(I-)]/[I+(I-)] ^[1]	Refined as inversion twin	Refined as inversion twin
Absolute structure parameter	-0.021 (8)	-0.013(5)	0.32(2)	0.10(2)

^[1] (Parsons, Flack and Wagner, Acta Cryst. B69 (2013) 249-259).

Computer programs: *CrysAlis PRO* 1.171.38.43 (Rigaku OD, 2015), *SHELXT* 2014/5 (Sheldrick, 2014), *SHELXL2018/3* (Sheldrick, 2018).

Table S2. Selected geometric parameters (Å, °)

	I (Mn 295 K)	II (Mn 120 K)	III (Co 295 K)	IV (Ni 250K)
M—O1	2.168 (4)	2.168 (2)	2.086 (4)	2.067 (4)
M—N1	2.347 (5)	2.337 (2)	2.225 (5)	2.180 (6)
M—N4	2.188 (4)	2.1877 (18)	2.091 (3)	2.050 (4)
M—N7 ⁱ	2.206 (4)	2.2017 (18)	2.118 (3)	2.079 (4)
M—N8	2.170 (3)	2.1717 (16)	2.083 (2)	2.044 (4)
M—N11 ⁱⁱ	2.185 (3)	2.1971 (17)	2.103 (3)	2.064 (4)
O1—M—N1	178.41 (11)	178.43 (6)	179.03 (11)	178.80 (17)
O1—M—N4	93.29 (16)	94.18 (7)	92.13 (16)	93.2 (2)
O1—M—N7 ⁱ	93.99 (18)	94.03 (8)	93.30 (19)	91.3 (2)
O1—M—N8	95.38 (17)	95.77 (8)	89.54 (19)	88.0 (2)
O1—M—N11 ⁱⁱ	90.06 (18)	90.90 (7)	87.70 (17)	175.0 (3)
N4—M—N1	86.98 (17)	86.67 (8)	174.1 (2)	91.53 (18)
N4—M—N7 ⁱ	172.3 (2)	171.30 (9)	92.02 (13)	87.4 (2)
N7 ⁱ —M—N1	85.67 (18)	90.56 (7)	86.84 (19)	93.5 (2)
N8—M—N1	86.17 (17)	85.06 (8)	93.67 (17)	87.5 (3)
N8—M—N4	91.21 (13)	85.54 (8)	87.29 (18)	91.35 (16)
N8—M—N7 ⁱ	90.68 (13)	90.71 (6)	90.65 (12)	90.42 (15)
N8—M—N11 ⁱⁱ	173.9 (2)	91.33 (6)	91.18 (11)	175.6 (2)
N11 ⁱⁱ —M—N1	88.37 (18)	173.10 (9)	175.75 (19)	89.7 (2)
N11 ⁱⁱ —M—N4	91.24 (14)	87.76 (8)	89.5 (2)	89.3 (2)
N11 ⁱⁱ —M—N7 ⁱ	86.17 (14)	86.43 (7)	85.84 (12)	86.45 (17)
Polyhedral volume	14.33 Å ³	14.32 Å ³	12.62 Å ³	11.98 Å ³
Distortion index	0.021	0.019	0.0170	0.016
Bond variance	angle 10.82 deg. ²	13.04 deg. ²	6.85 deg. ²	5.41 deg. ²

Symmetry code(s): (i) $x-1/2, -y+1/2, z$; (ii) $x, y-1, z$.

Table S3. Selected hydrogen-bond parameters

T(K)	$D-H\cdots A$	$D-H$ (Å)	$H\cdots A$ (Å)	$D\cdots A$ (Å)	$D-H\cdots A$ (°)
I	$O1-H1\cdots N2^i$	0.90	1.96	2.847 (6)	171.7
	$O1-H2\cdots N3^{ii}$	0.90	1.90	2.752 (6)	157.8
II	$O1-H1\cdots N2^i$	0.92	1.97	2.863(3)	164.7
	$O1-H2\cdots N3^{ii}$	0.91	1.86	2.760(3)	169.8
III	$O1-H1\cdots N2^i$	0.90	1.99	2.877(6)	167.2
	$O1-H2\cdots N3^{ii}$	0.90	1.90	2.766(6)	161.6
IV	$O1-H1\cdots N3^i$	0.88	1.91	2.764 (7)	163.3
	$O1-H2\cdots N2^{ii}$	0.88	2.03	2.895 (8)	168.1

Symmetry code(s): (i) $-x+1/2, y-1/2, z+1/2$; (ii) $-x+1/2, y+1/2, z+1/2$.

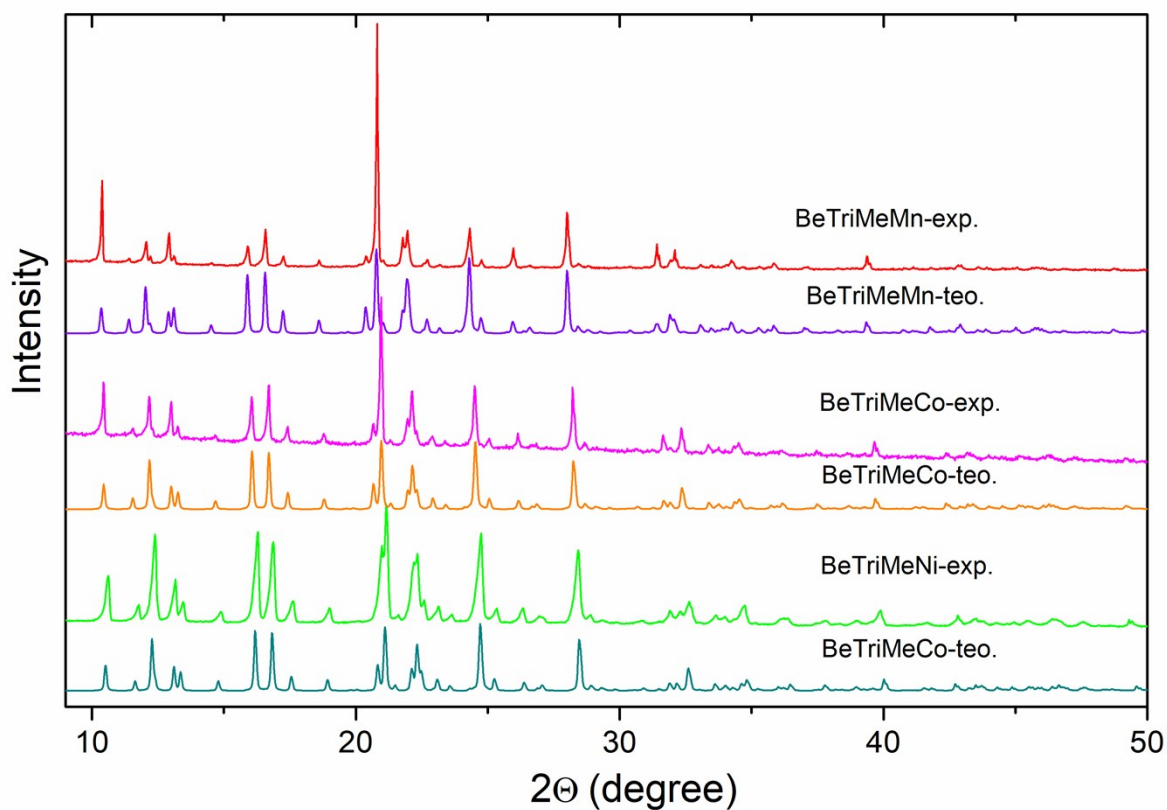


Figure S1. Room-temperature powder XRD patterns for the as-prepared BeTriMeM samples (M=Mn, Co, Ni) together with the calculated ones based on the single crystal structure.

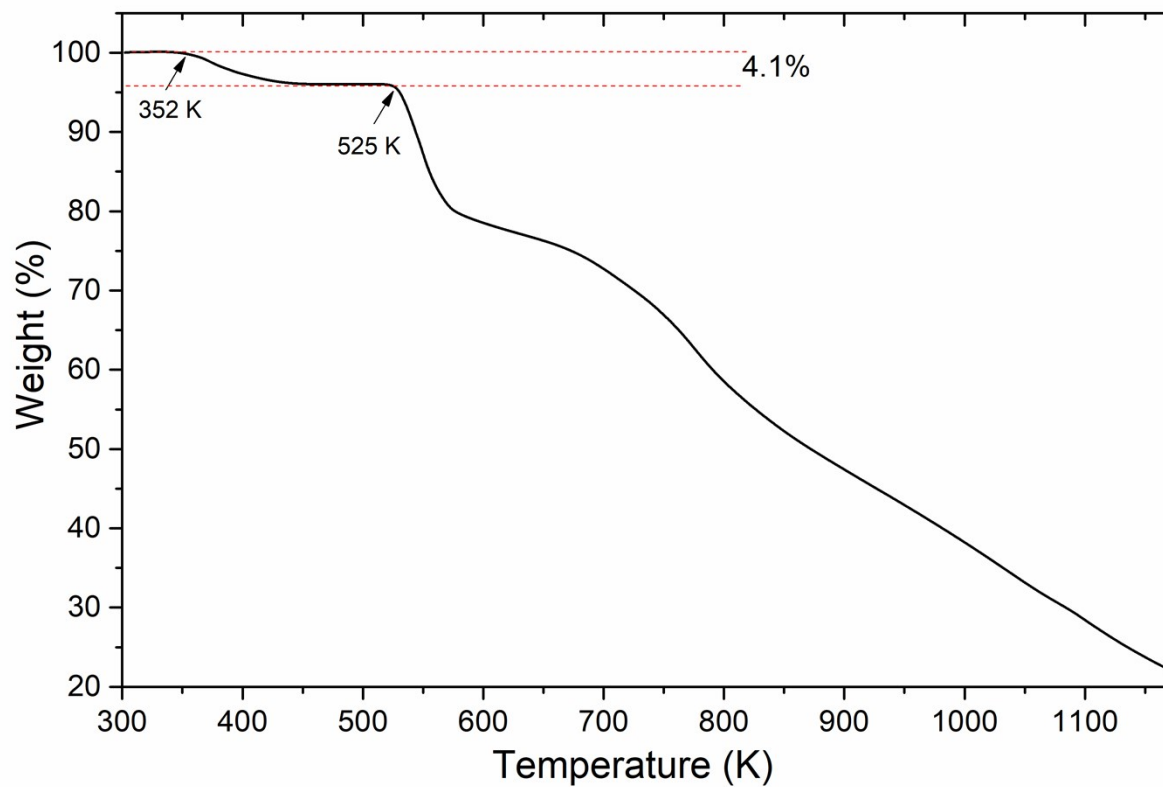


Figure S2. TGA plot of BeTriMeMn.

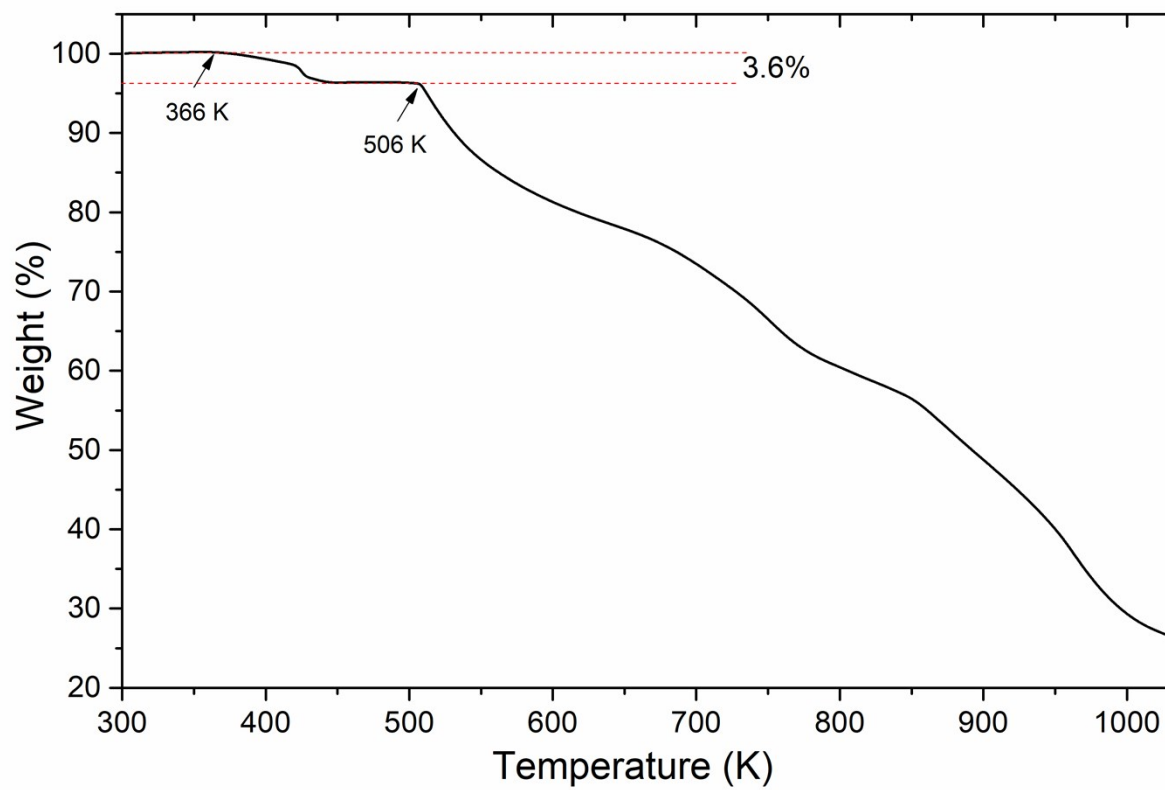


Figure S3. TGA plot of BeTriMeCo.

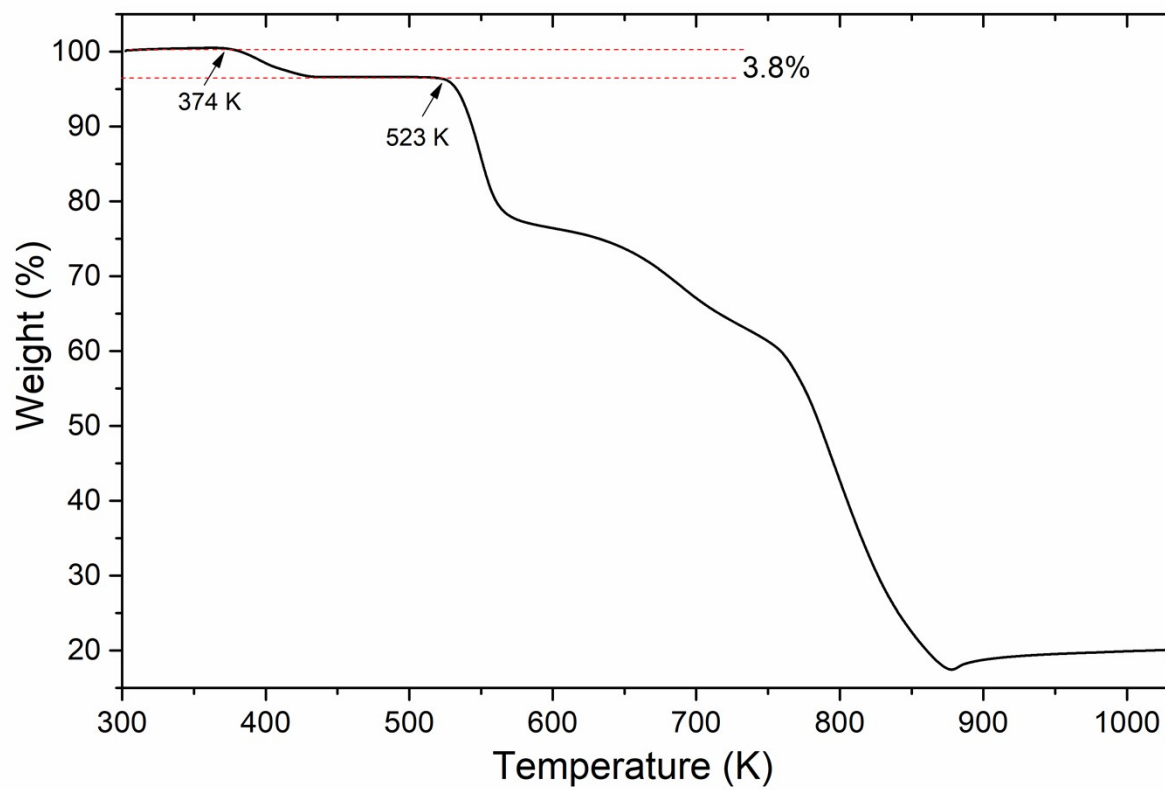


Figure S4. TGA plot of BeTriMeNi.

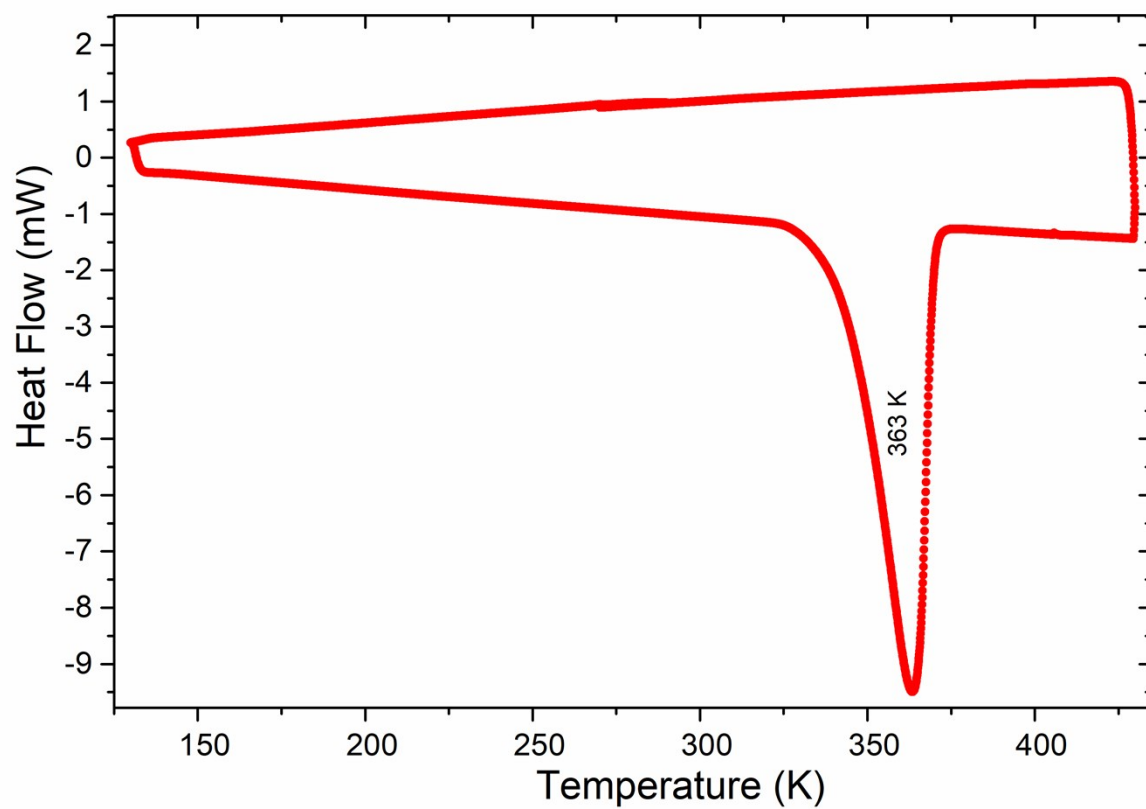


Figure S5. DSC trace for BeTriMeMn: cooling from 290 K to 130 K, heating to 430 K and cooling to 270 K.

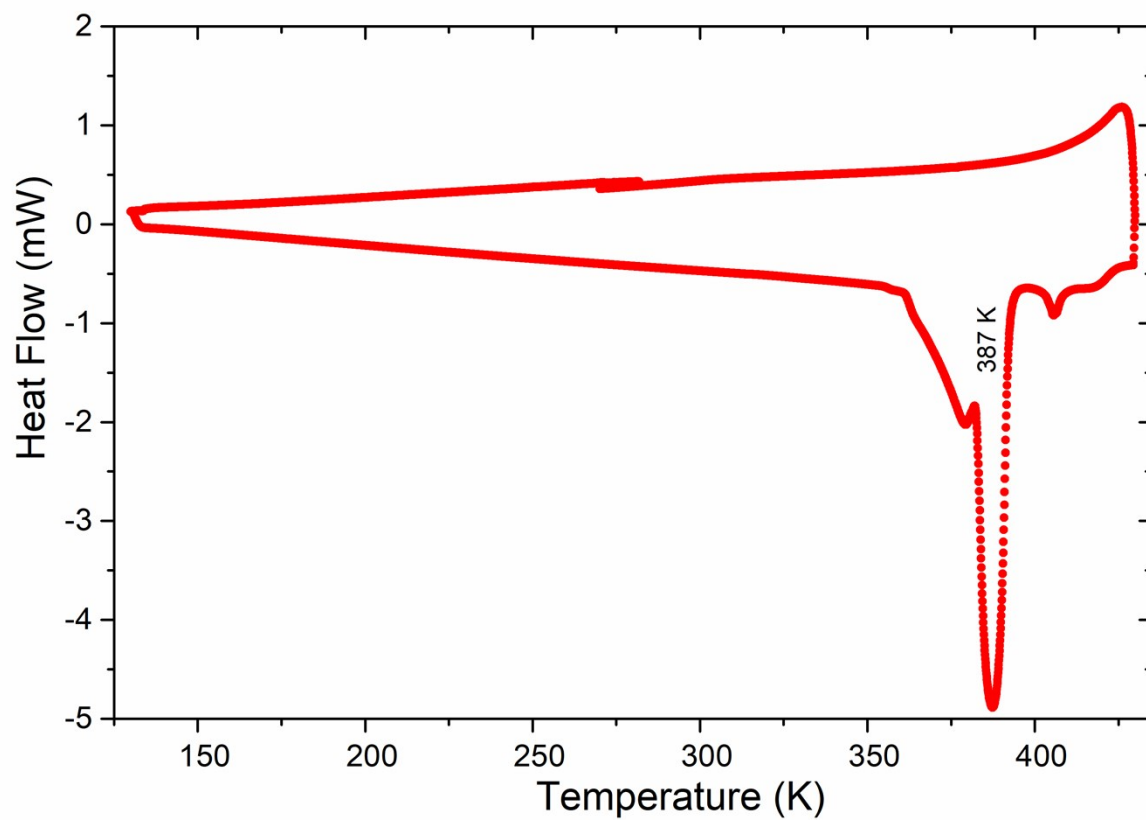


Figure S6. DSC trace for BeTriMeCo: cooling from 282 K to 130 K, heating to 430 K and cooling to 270 K.

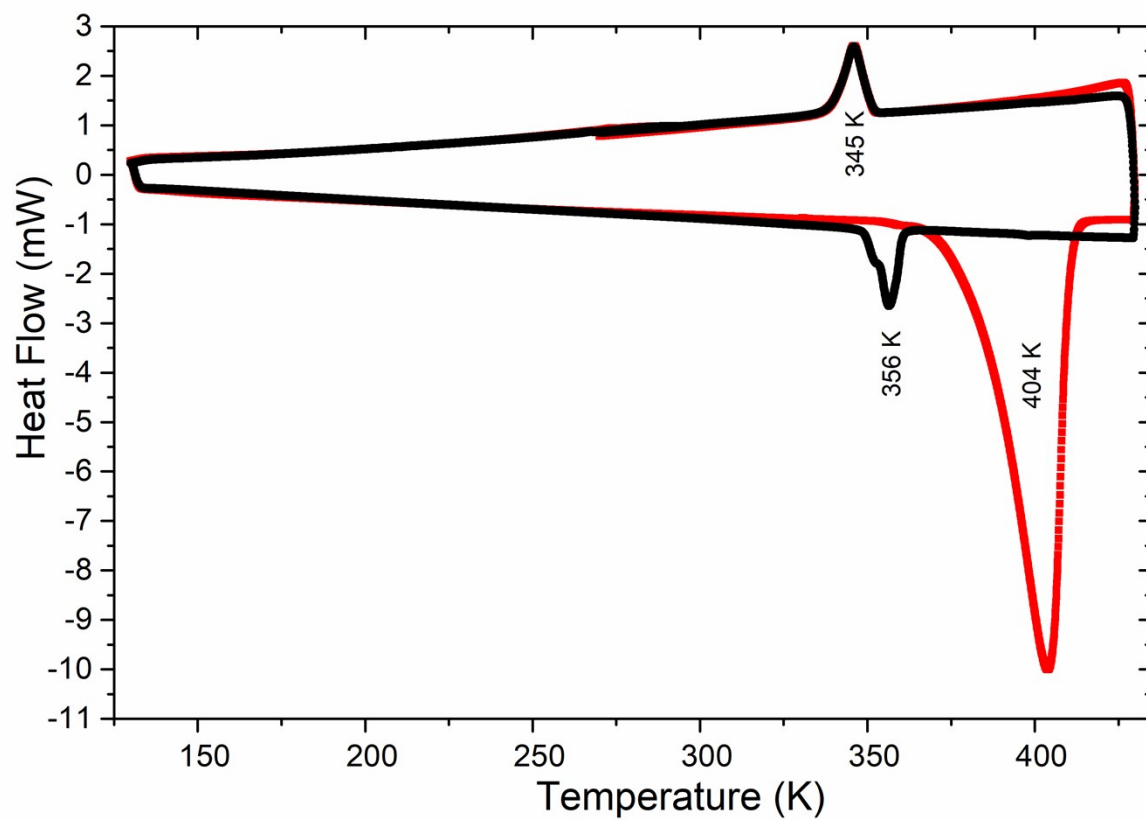


Figure S7. DSC traces for BeTriMeNi: cooling from 295 K to 130 K, heating to 430 K and cooling to 270 K (1st run, red line; 2nd run, black).

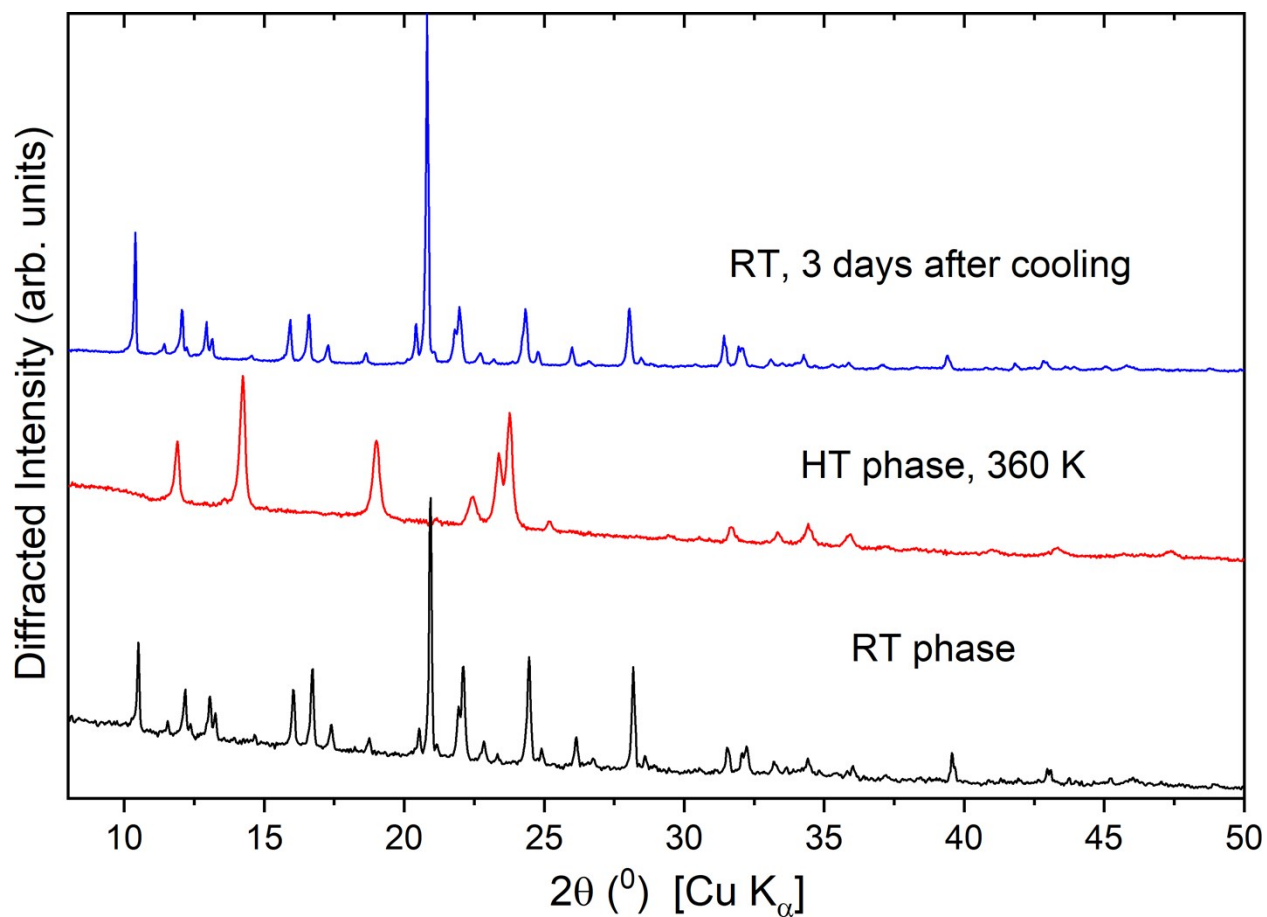


Figure S8. The PXRD of the RT and HT anhydrous phase of BeTriMeMn as well as the heat-treated sample kept for three days at RT. The anhydrous phase may be indexed in the orthorhombic unit cell with $a=18.378(4)$ Å, $b=11.422(4)$ Å, $c=8.109(5)$ Å. The crystallite size, calculated from the Scherrer formula after the structural transformation equals around 40 nm.

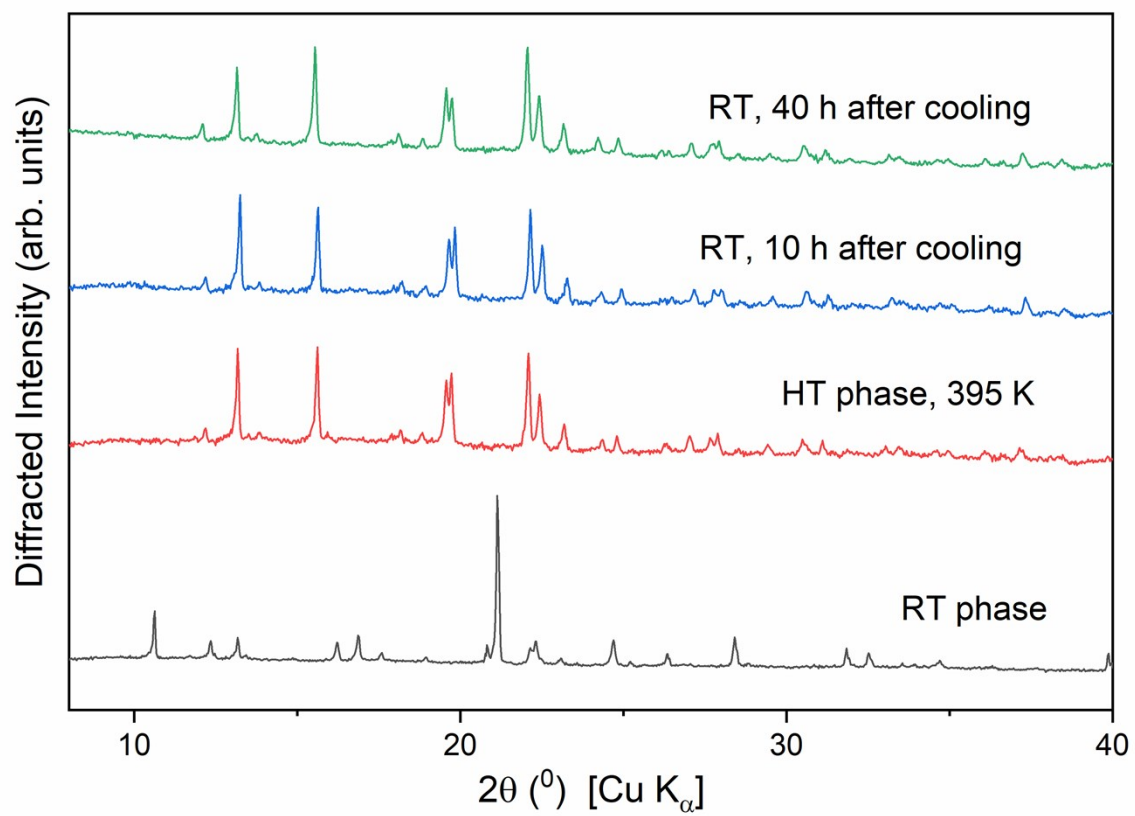


Figure S9. The PXRD of the RT and HT anhydrous phase of BeTriMeCo as well as the heat-treated sample kept for 10 and 40h at RT.

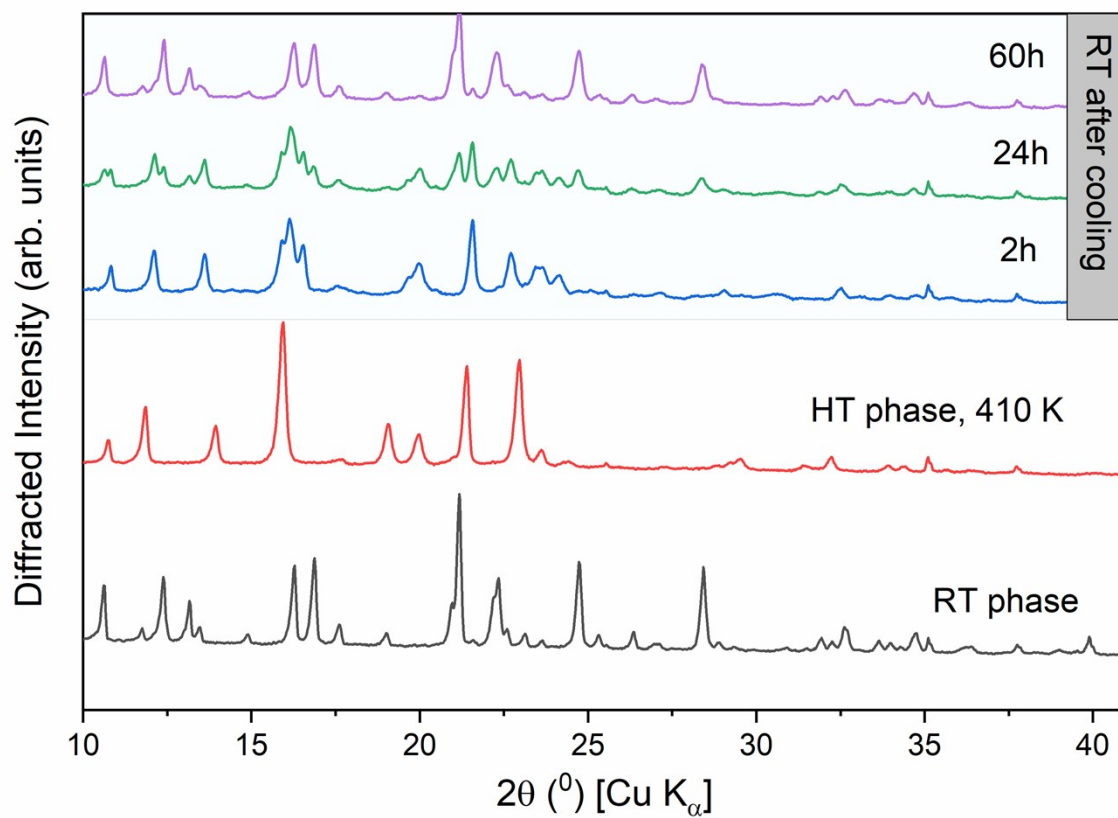


Figure S10. The PXRD of the RT and HT anhydrous phase of BeTriMeNi as well as the heat-treated sample kept for 2, 24 and 60h at RT.

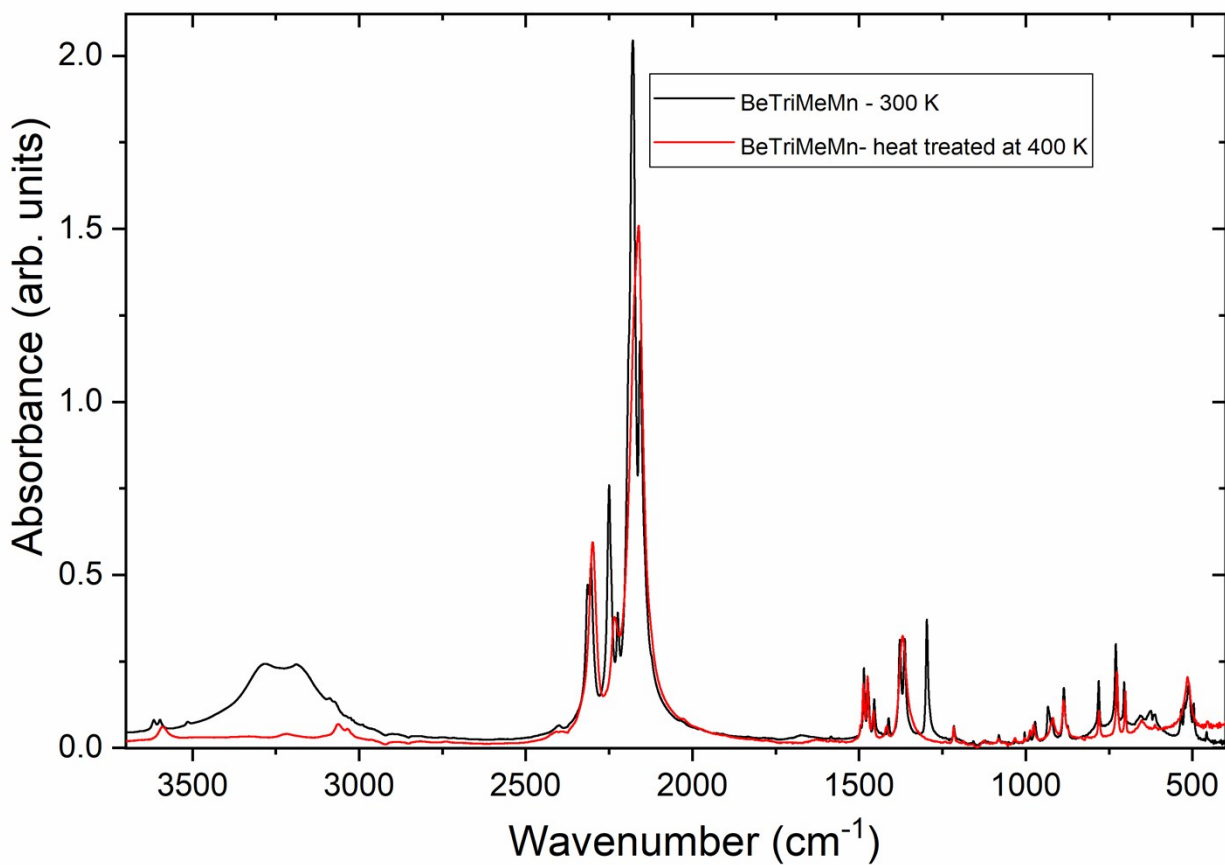


Figure S11. IR spectra of the original BeTriMeMn sample and the same sample heat-treated at 400 K.

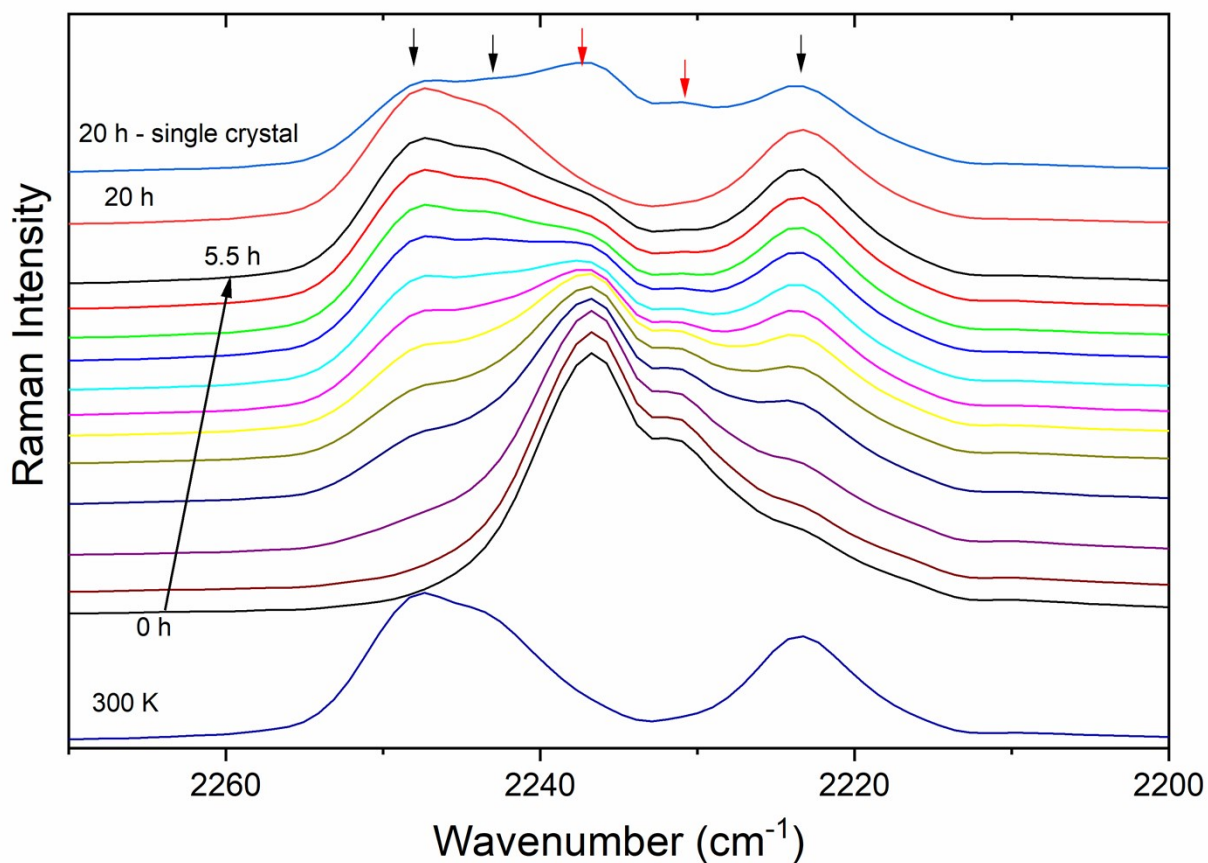


Figure S12. Raman spectrum of the powdered BeTriMeMn crystals (330 K) and the same powder heat treated at 400 K, cooled to RT and kept for 0-5.5 h. For the comparison sake, Raman spectrum recorded for a sample prepared by grinding a small single crystal (less than 1 mm) that was heat-treated at 400 K and left at RT for 20h is also shown. Black (red) arrows indicate bands characteristic for hydrated (anhydrous) phase.

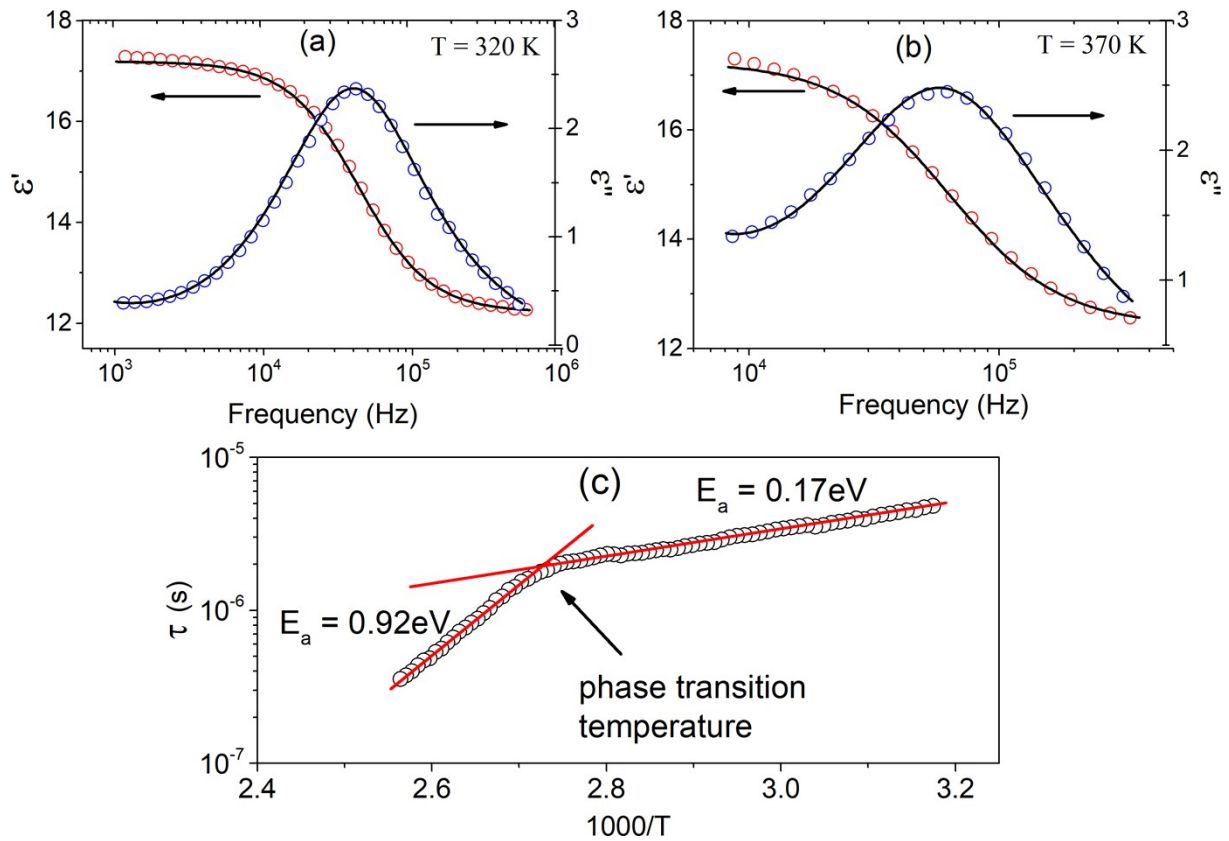


Figure S13. Frequency dependence of (a) imaginary and (b) real components spectra of complex dielectric permittivity. Solid lines represents the HN fitting.(c) Relaxation map, τ as a function of $1000/T$.

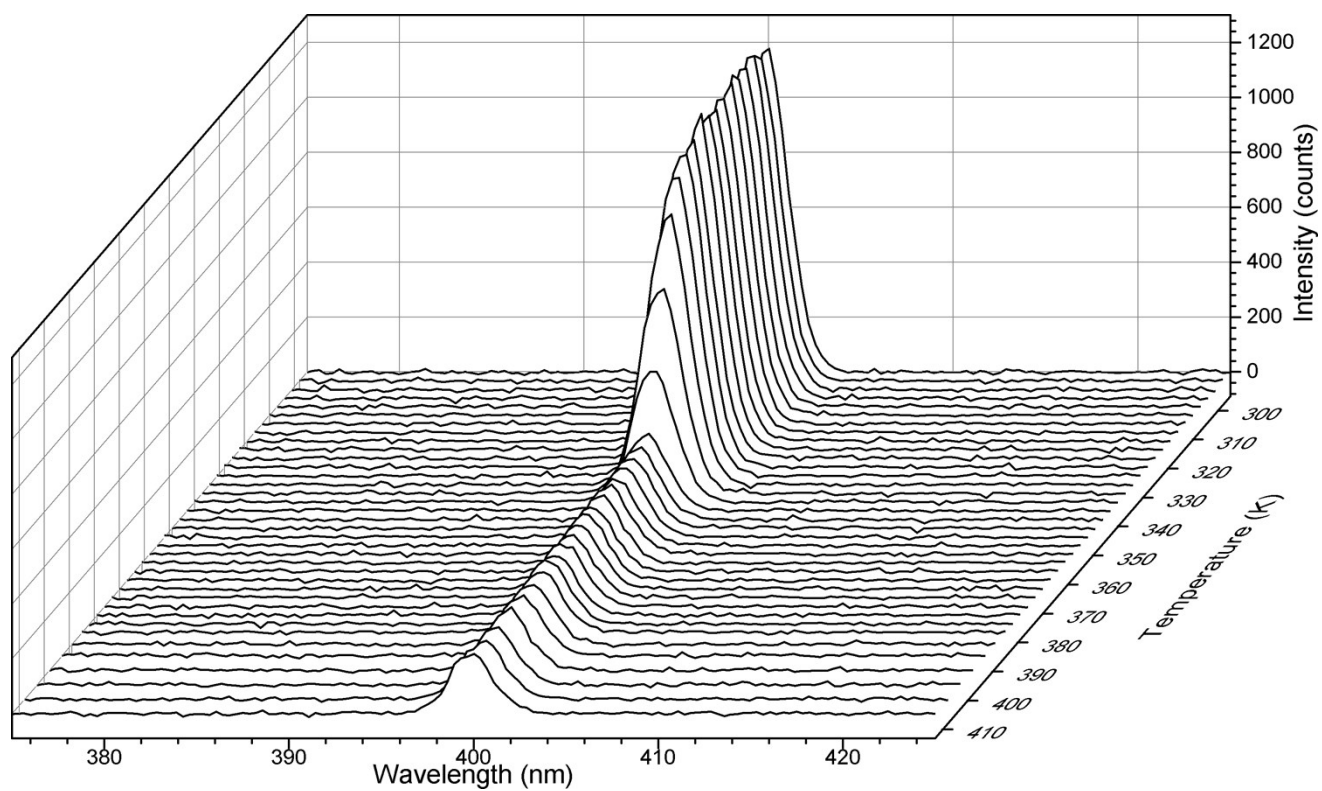


Figure S14. SHG spectra obtained upon irradiation with 800 nm femtosecond laser pulses of BeTriMeMn during heating cycle (295K to 413K).

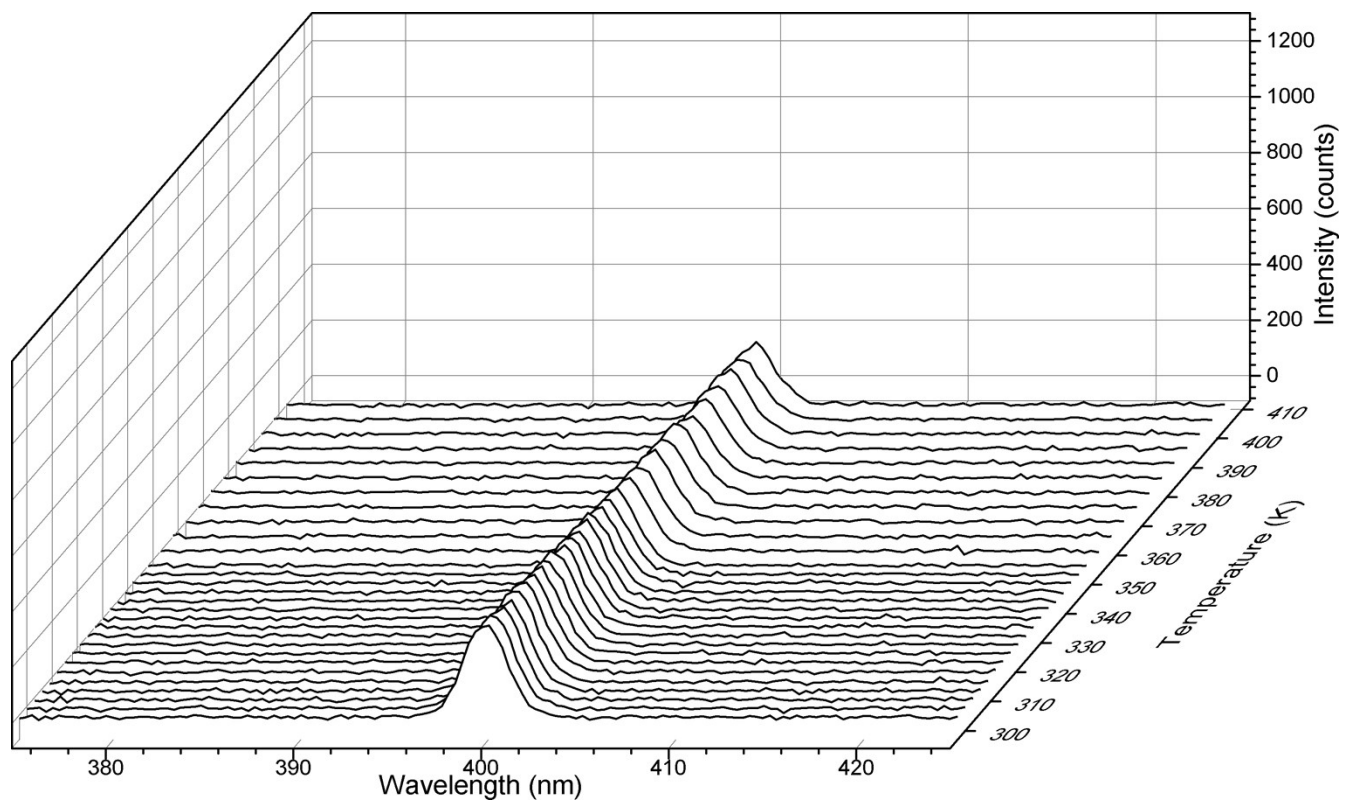


Figure S15. SHG spectra obtained upon irradiation with 800 nm femtosecond laser pulses of BeTriMeMn during cooling cycle (413K to 297K).

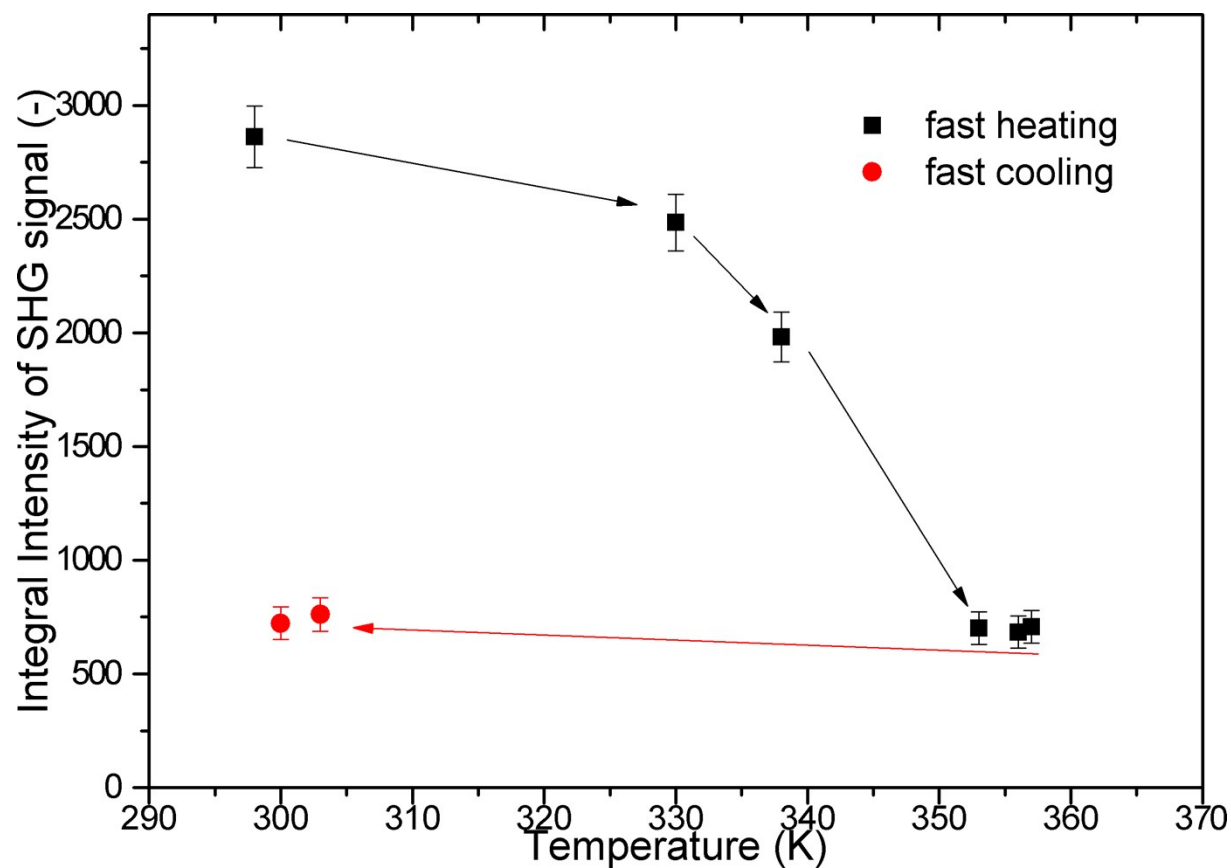


Figure S16. Plot of integral intensities of SHG signal of BeTriMeMn for fast heating and cooling runs.

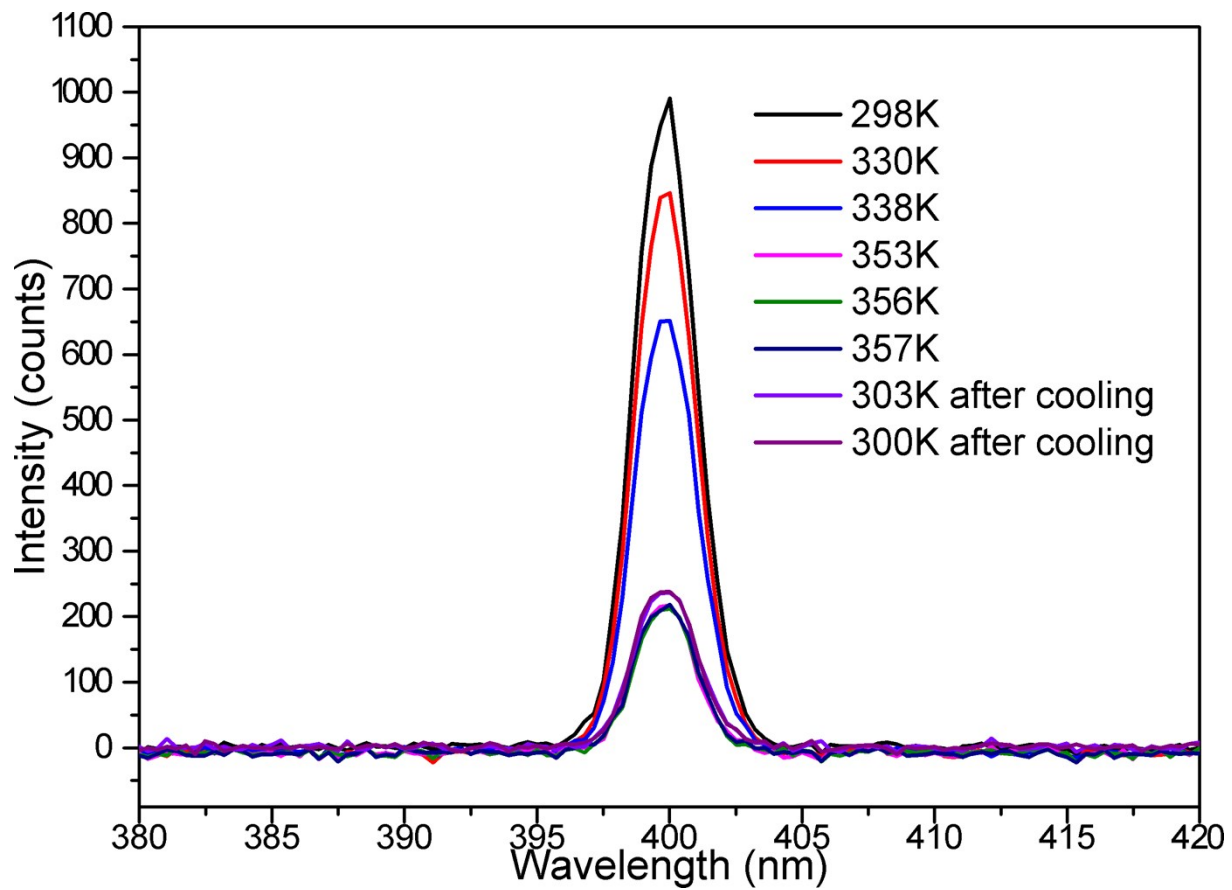


Figure S17. Overlay of experimental spectra of BeTriMeMn for fast heating and cooling runs.

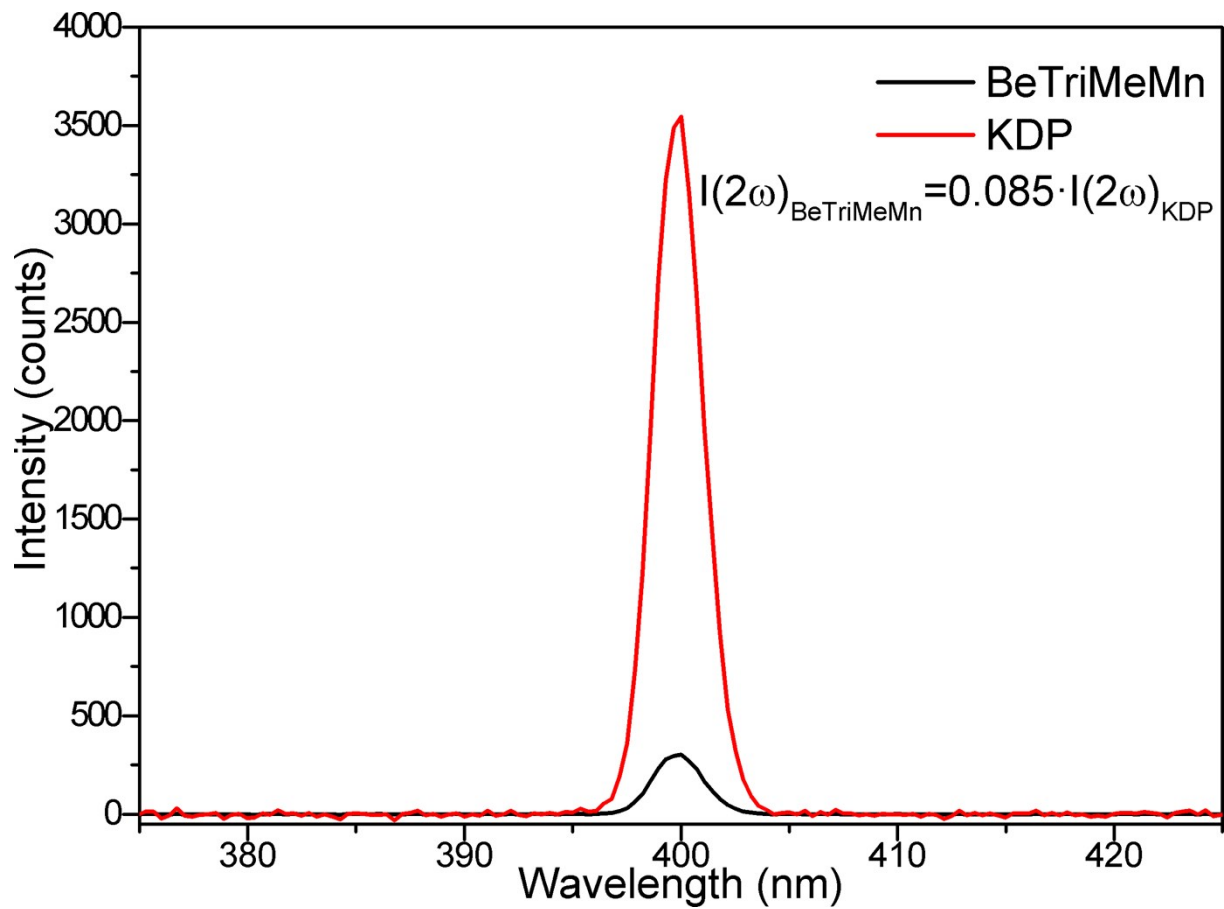


Figure S18. SHG traces for BeTriMeMn (red) and that of KDP (black) obtained upon irradiation with 800 nm femtosecond laser pulses at 295K.

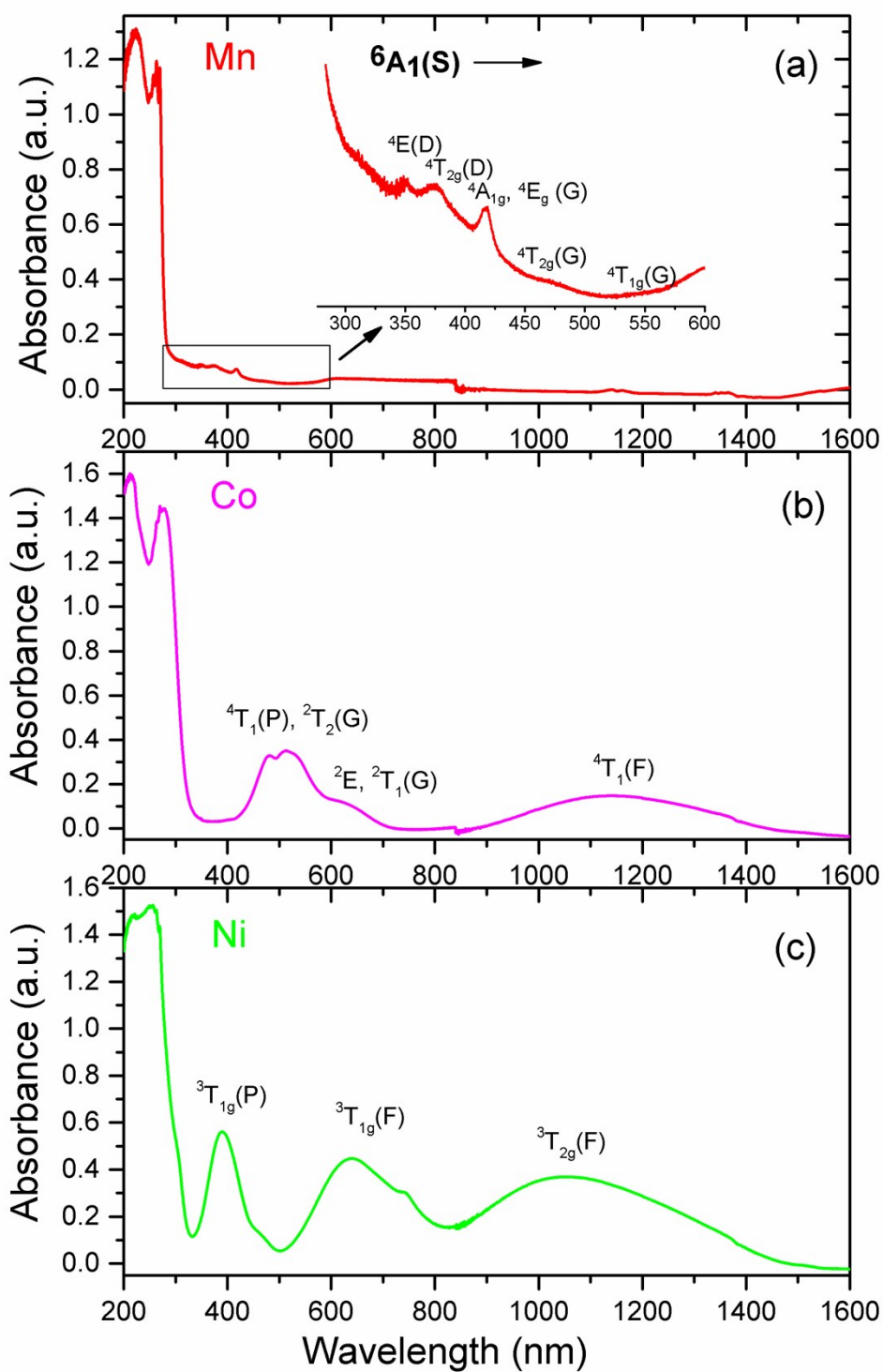


Figure S19. Absorption spectra of a) BeTriMeMn b) BeTriMeCo and c) BeTriMeNi recorded at 300 K.

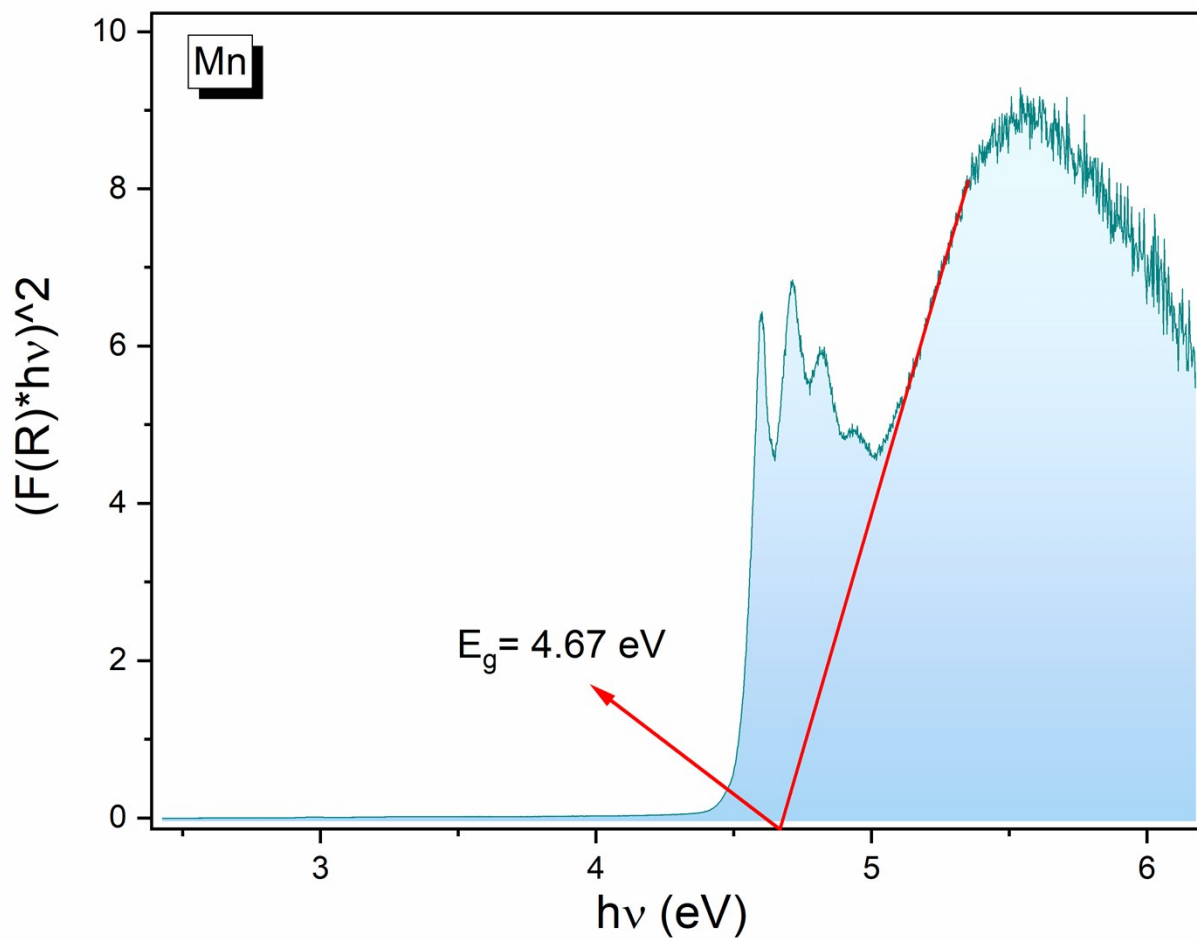


Figure S20. The energy band gap of BeTriMeMn determined using Kubelka – Munk function.

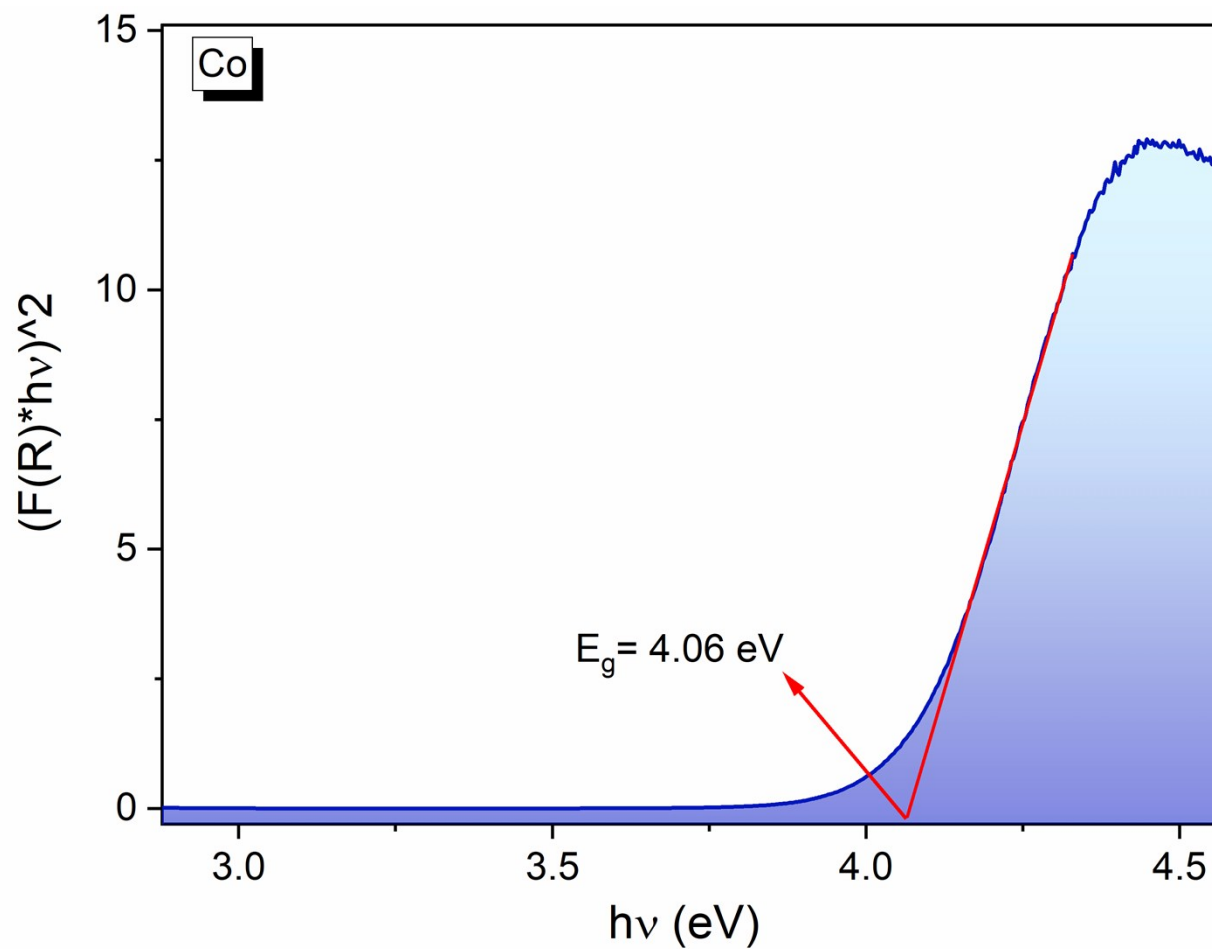


Figure S21. The energy band gap of BeTriMeCo determined using Kubelka – Munk function.

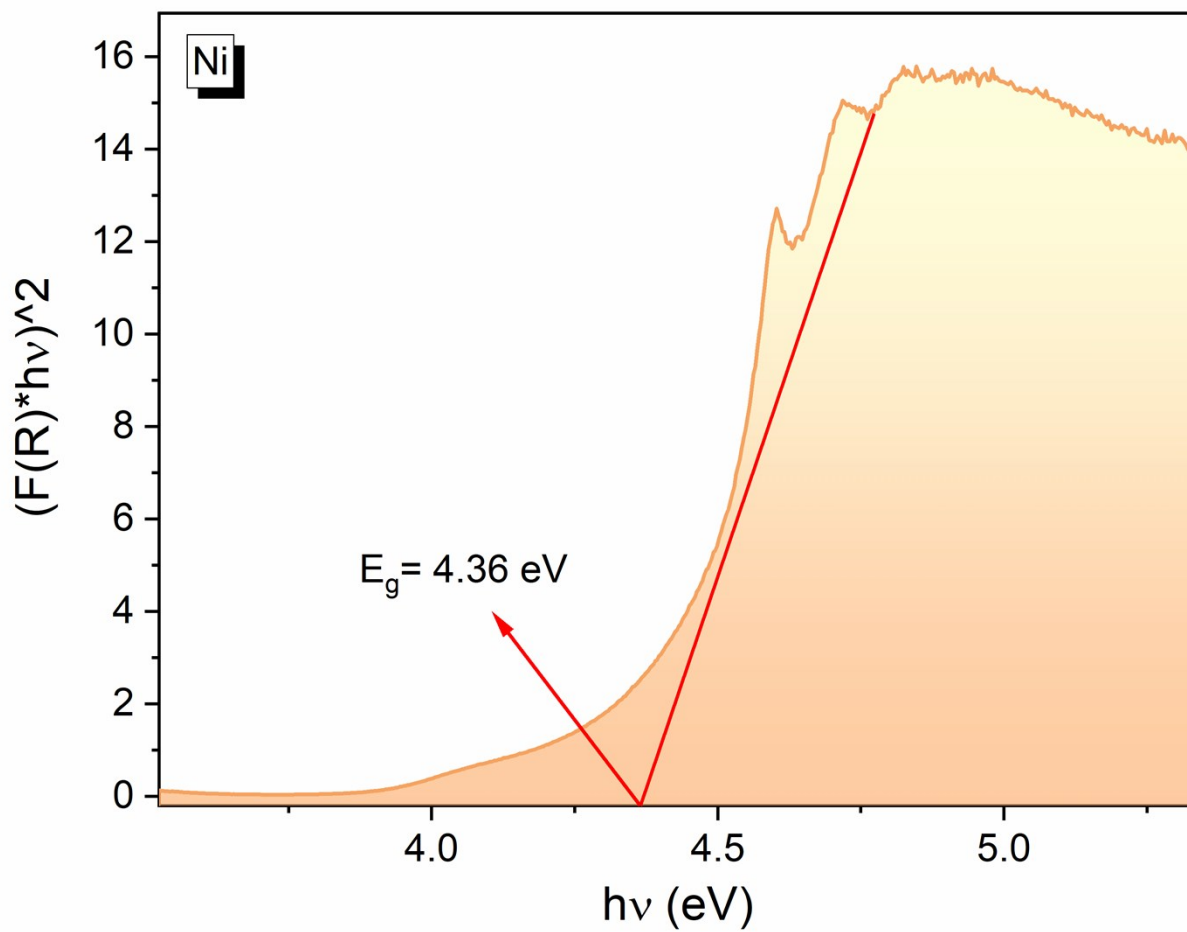


Figure S22. The energy band gap of BeTriMeNi determined using Kubelka – Munk function.

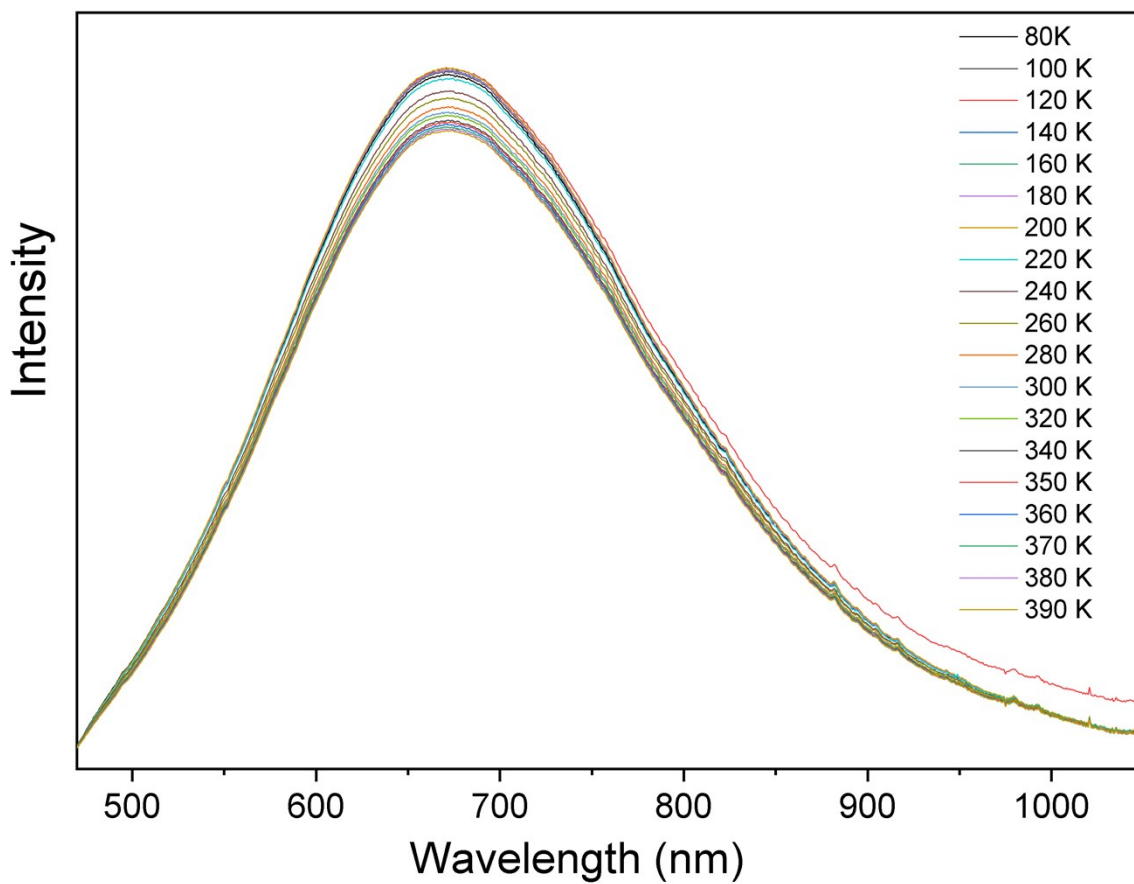


Figure S23. The temperature dependent emission spectra of anhydrous BeTriMeMn excited at 450 nm.

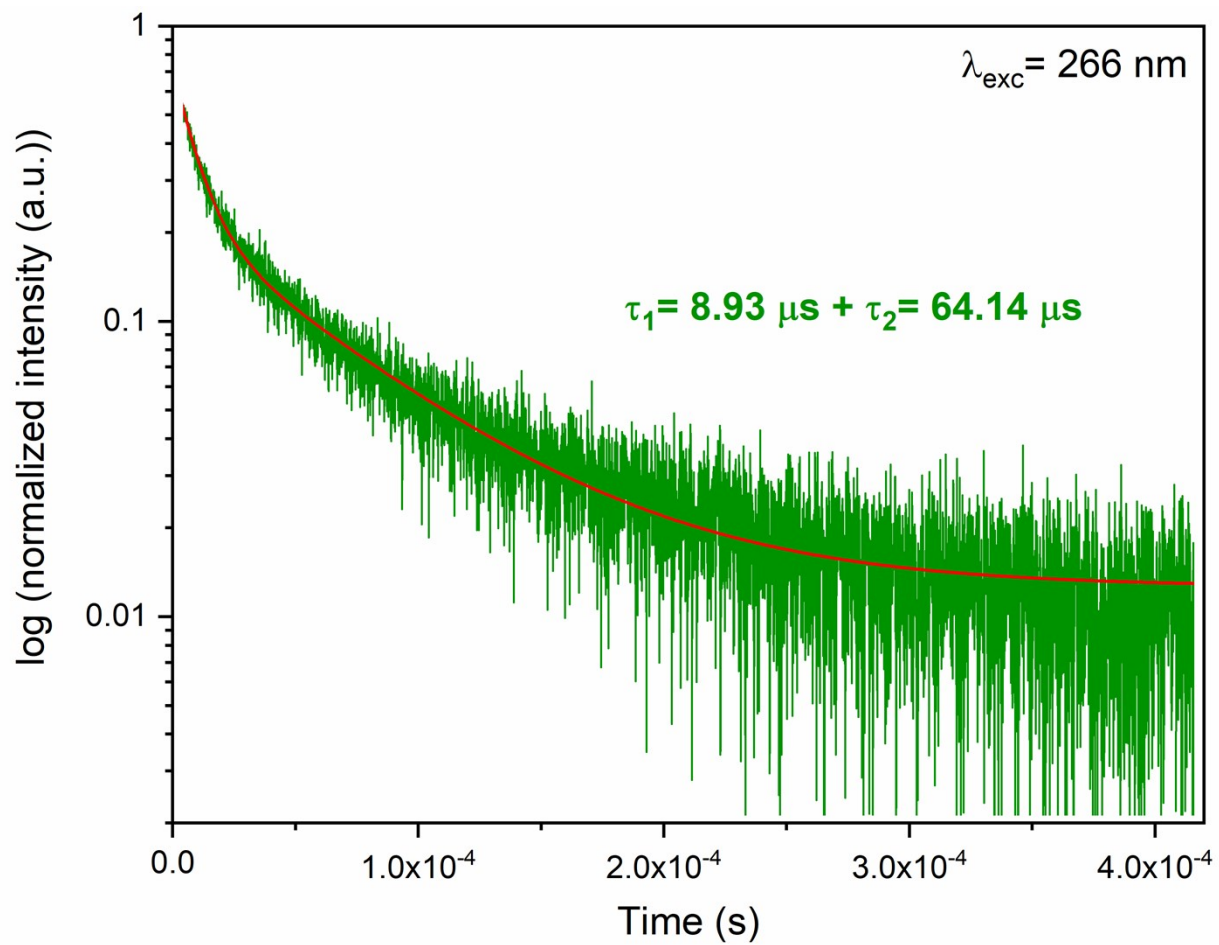


Figure S24. Emission decay curve of BeTriMeMn 300 K.